Chapter 1

Introduction of the Sun, Waves and Quasi-Periodic Pulsations

In this chapter, we provide a simple overview of the Sun and its atmosphere, including its interior and how energy is generated in the core and then transferred to the surface. We also briefly describe the Sun's global oscillations and touch upon the origin of its magnetic field. Moving to the outer layers, we discuss about the different layers of the solar atmosphere. Since our thesis focuses on studying the waves and quasi-periodic pulsations (QPPs) in the solar atmosphere, we delve into a description of these phenomena upto some extent. This includes discussing various types of wave modes in the magnetized solar atmosphere and the physical conditions under which these waves propagate. We also describe observational evidence of waves in different magnetic structures such as the quiet Sun and active region sunspots. Furthermore, we describe the observational signatures of QPPs in the solar corona and various mechanisms and models proposed to explain their physical origin. At the end, we outline the summary of various chapters of the present thesis.

1.1 Overview of the Sun

Our nearest star, the Sun, falls into the category of G-type main-sequence stars and boasts a surface temperature of around 5,800 K. It resides within one of the spiral arms of the Milky Way, our own galaxy, formed through the compression of interstellar clouds during its rotation, a balance between gravity and pressure gradient forces. Roughly 4.6 billion years ago, the Sun formed due to gravitational collapse of a molecular cloud. Despite being located at a staggering distance of 1.5×10^8 km, recent advancements in observational instruments have significantly improved our understanding about the Sun and its various plasma processes. Solar physics has played a pivotal role in numerous scientific breakthroughs over the past century. The temperature of the Sun's atmosphere is so intense that subatomic particles struggle to form neutral atoms, resulting in a plasma composed of fully ionized electrons and nuclei. This plasma, carrying an electric charge, can conduct electricity and generate a magnetic field. Scientists delve into the complex interaction between this magnetic field and plasma movement through a field called magnetohydrodynamics (MHD). Understanding this interaction is crucial to comprehend phenomena like solar eruptions, heating and transients.

The Sun consists of various layers, including the corona, its hottest and outermost layer, where temperature in is million-degree kelvin. Similar to other stars, the Sun is a colossal sphere of intensely hot, predominantly ionized gas, emitting energy independently. It dwarfs Earth in size, with enough volume to hold approximately 1.3 million Earths. Although lacking a solid surface or core, the Sun exhibits layered structures both in its interior and exterior. These layer undergoe significant changes in its interior and exterior, marked by origin and transport of magnetic field and plasma as well as dynamic and violent eruptions in its outer layers. The fundamental properties of the Sun are described in Table 1.1.

Table 1.1: The Physical Properties of the Sun (Credit: Priest 2014)

Physical Parameters	Physical Quantity
Age	4.6×10^9 years
Solar mass	1.99×10^{30} kg ($\approx$ 330 times of the Earth)
Solar radius	695.5 Mm (6.955×10^8 m)
Solar mean density	1.4×10^3 kg m^{-3}
Photospheric temperature	5785 K
Solar surface gravity	274 m s^{-2}
Escape velocity at solar surface	618 km s^{-1}
Equatorial rotation period	26.24 days
Luminosity (Radiation)	3.86×10^{26} W
Mass-loss rate	10^9 kg s^{-1}
Angular momentum	1.7×10^{41} kg m$^2 s^{-1}$
1 arcsec	$\approx$ 726 km

The behavior of plasma inside and outside the Sun significantly impacts space weather and our daily lives. The Sun serves as a vast laboratory in space, enabling us to closely study its physics and expand our knowledge. Its atmosphere, primarily composed of gases like hydrogen (about 92%) and helium (about 8%), with small amounts of other elements such as carbon, oxygen, and nitrogen, etc, which is a typical for the stars in general (Asplund et al., 2009). The Sun is divided into two main parts: the interior and the exterior. A schematic diagram depicting the different parts of the Sun is shown in Figure 1.1. Inside, there is a core at the center where nuclear reactions produce energy, which then moves outward as light and heat through layers called radiation and convection zone. The Sun's exterior is characterized by different layers of the magnetic atmosphere.

1.1.1 Solar interior

The solar interior comprises three distinct layers. Firstly, there is the core, where continuous thermonuclear reactions occur, producing the energy. This region is intensely hot, with temperature there is 15 million Kelvin, and it is densely packed with ionized material, generating most of the Sun's energy through hydrogen fusion. Moving outward from

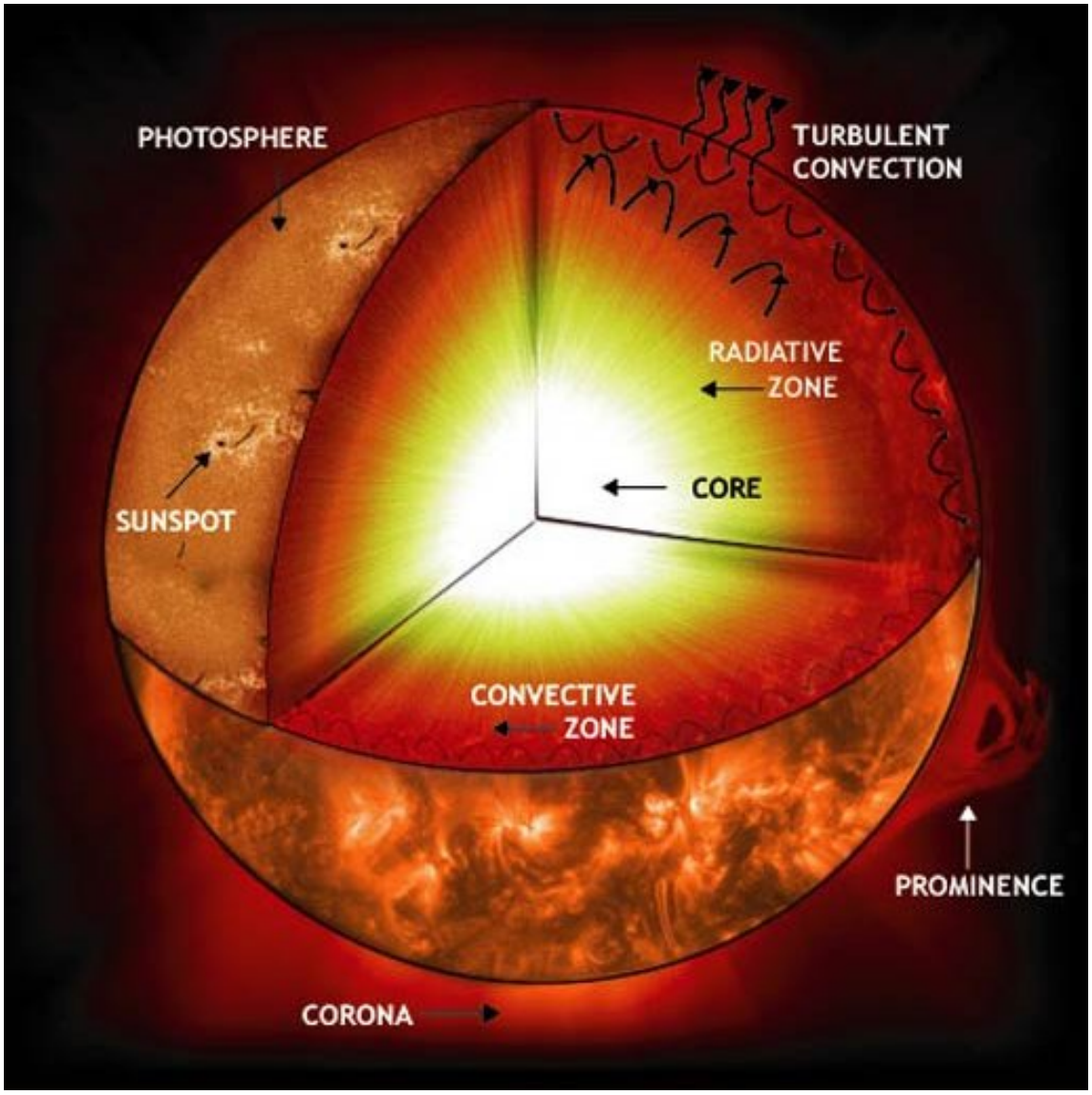

Figure 1.1: The image illustrates various parts of the Sun, commencing from the core where energy generation occurs, and extending outward across the radiation and convection zones. It further depicts the Sun's surface, known as the photosphere, and its outermost layer, the corona. Additionally, the picture showcases several phenomena within the Sun's atmosphere, including loops, sunspots, and prominences. (Credit: NASA/Berkeley - SSL).

the core, we encounter the radiative zone. Here, energy from the core travels outward in the form of electromagnetic radiation, but the journey is slow due to the dense medium. The photons interact numerous times, causing delays of hundreds of thousands of years before reaching to the next layer. The third layer is the convection zone, a dense region extending about 2×10^5 Km. Energy moves outward through this zone as rising plasma blobs, resembling the convection cells. The gas temperature is lower here, but opacity increases, leading to instability (e.g., Schwarzschild, 1906; Thorne, 1966). Hot gas rises, cools at the surface, and descends, forming a continuous cycle.

Direct observation of the solar interior is impossible due to its opacity. Instead, we rely on solar seismology and neutrino observations for information (Basu, 2016). The Sun functions as a colossal fusion reactor, where hydrogen atoms fuse into helium, releasing energy outward. Despite its immense mass, the Sun does not implode, thanks to outward pressure from core reactions making it in hysrostatic equilibrium. The Sun's inner core is completely concealed and can only be examined using helioseismology, despite the fact that its surface radiates and is visible. Nonetheless, the physical conditions within the Sun may be inferred from equations describing its structure and boundary conditions provided by observations.

Generation of energy at core and transportation to the surface

While we can not directly explore the Sun's inner layers because of the thick, cloudy plasma called the photosphere, we can still learn about its properties. Understanding how temperature and pressure change as we go deeper into the Sun is the main challenge in studying its structure. These changes are controlled by equations that keep everything in mechanical and thermal balance. Mechanical balance means the pressure inside the Sun pushes outwards, counteracting the inward pull of gravity (see, Cox and Giuli, 1968; Priest, 2014).

The equation for this balance looks like this (Chitre and Dwivedi, 2008):

$$\frac{dP(r)}{dr} = -\frac{GM(r)}{r^2}\rho(r), \tag{1.1}$$

and

$$\frac{dM(r)}{dr} = 4\pi r^2\rho(r), \tag{1.2}$$

In this equation, 'P(r)' represents the pressure, '$\rho(r)$' signifies the density and 'm(r)' denotes the the mass interior for a spherically symmetric Sun. The solar core generates nuclear energy, which is then radiated through the surface of the Sun to maintain thermal equilibrium. This equilibrium guarantees that the Sun's luminosity, representing the energy it emits, is offset by the nuclear energy generated within its interior and given as (Chitre and Dwivedi, 2008)

$$\frac{dL(r)}{dr} = 4\pi r^2\rho(r)\epsilon, \tag{1.3}$$

Here, 'ϵ' denotes the nuclear energy produced per unit mass. The expression $L(r) = 4\pi r^2(F_{\text{rad}} + F_{\text{conv}})$ represents the Sun's luminosity, which comprises the combined fluxes of radiation and convection. Solar energy originates primarily from hydrogen fusion reactions within the central core, where conditions favor thermonuclear fusion. The primary reaction pathways for stellar (including solar) fusion are governed by two pathways, with the pp-chain reaction being considered the most probable due to the abundance of hydrogen and the low nuclear charge. The pp-chain reaction generates approximately 98% of the Sun's energy, while the remaining 2% originates from the CNO cycle.

The overall pp-chain reaction is as follows:

$$4\,1H \rightarrow {}^4He + 2e^+ + 2\nu_e + 2\gamma + 26.7\ (inMeV) \tag{1.4}$$

That is, four protons combine to create a single helium nucleus, accompanied by the emission of two neutrinos and the liberation of energy, which is transmitted through gamma rays. The rate of energy production can be represented by a straightforward power law or more complex formulae that account for nuclear reaction rates. These generated neutrinos in the nuclear reaction exit the Sun's interior without obstruction since they do not interact with its opaque material. The energy generated through nuclear fusion reactions within the Sun's central core is transmitted outward in form of $\gamma-$rays. Nevertheless, the dense solar material causes opacity, hindering the smooth transmission of energy produced in the core. As a result, photons undergo repeated absorption and emission by the gas present within the radiative zone. This process involves various mechanisms, such as transitions between bound states (bound-bound), transitions from bound to free states (bound-free or photoionization), transitions between free states (free-free), and scattering [1].

It takes approximately 1.7×10^5 years for the energy to diffuse outward to the bottom of the convection zone, situated at approximately 0.71 times the solar radius $R_\odot$. Here, the temperature declines from 15 million Kelvin at the core to around 2 million Kelvin. The radiative flux (F_{rad}) is related to the temperature gradient as (Chitre and Dwivedi, 2008)

$$F_r = -\frac{4acT^3}{3\kappa\rho}\frac{dT}{dr}, \tag{1.5}$$

[1] https://astro.ru.nl/ onnop/education/stev_utrecht_notes/chapter5-6.pdf

In this equation, 'a' represents the Stefan-Boltzmann constant, 'c' symbolizes the speed of light, and 'κ' denotes the opacity of solar material. This opacity arises from numerous atomic processes involving different elements and various ionization stage (e.g., Iglesias and Rogers, 1996; Rogers and Iglesias, 1992).

The outermost layer of the Sun's interior is known as the convective envelope. It is cooler and less translucent than the inner radiative envelope. As we move outward from the radiative zone, the efficiency of energy transfer through radiation decreases, and heat starts to accumulate. When the rate of temperature declining with radius surpasses what would occur without additional heat, convection becomes dominant. In such cases, upward-moving material becomes warmer than its surroundings, and it rises continuously. Beyond 0.75 times the solar radius ($R_\odot$), convection becomes the primary method of energy transfer. In contrast to radiation, convection rapidly transports energy through an opaque medium, with heated gas taking around 10 days to rise through the convection zone. Convection cells closer to the surface are smaller compared to those deeper within, and their upper parts are referred to as granules, observed at the solar surface (i.e.,photosphere) with a telescope. All energy from the convection zone is absorbed by the surface of the Sun, which is then emitted at a temperature of about 5800 Kelvin. At the visible surface, the density is remarkably low, approximately 2×10^{-7} gm cm^{-3}, about 1/10,000th the density of air at the sea level. Under these conditions, the Schwarzschild instability criterion (e.g., Choudhuri, 1998; Schwarzschild, 1906; Thorne, 1966) is met, and energy transport is mainly facilitated by convection, using a local mixing-length formulation (Böhm-Vitense, 1960; Chitre and Dwivedi, 2008) for modeling as follows:

$$F_c = -\kappa_t \rho T \frac{dS(r)}{dr}, \tag{1.6}$$

where κ_t is turbulent diffusivity, and S(r) is entropy of the system.

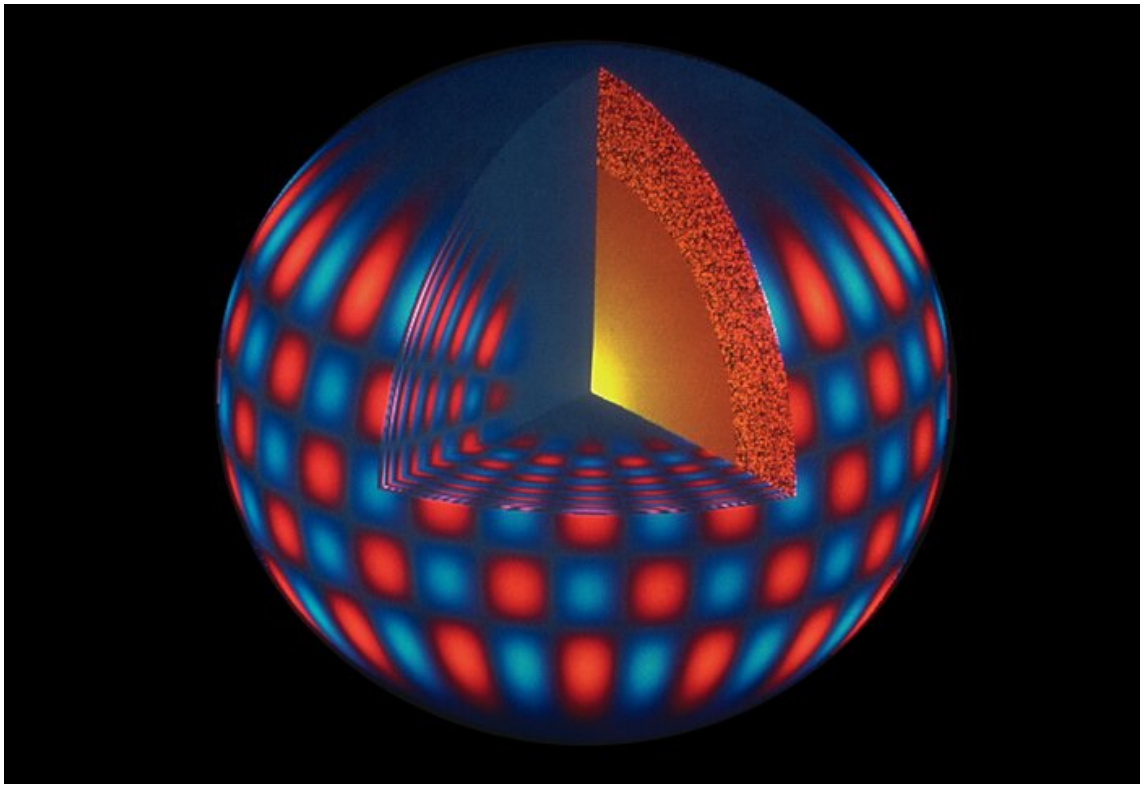

Figure 1.2: Sound waves within the sun cause the visible solar disk to oscillate inward and outward. This collective movement is a composite of countless oscillations, depicted here by regions pulsating inward (red areas) and outward (blue areas). By scrutinizing the frequencies of numerous modes and employing theoretical models, solar astronomers can glean valuable insights into the internal structure and dynamics of the sun (Credit: NSO/AURA/NSF).

Oscillations in the solar interior

The sun's inner layers remain hidden due to its high opacity at the photospheric level, making it challenging to study its internal structure directly. However, scientists have used mathematical models and various indicators like energy flux, neutrinos, and solar oscillations to gain insights into the solar interior (e.g., Basu, 2016; Duvall and Harvey, 1983; Guenther and Demarque, 1997; Libbrecht et al., 1990; Turck-Chièze and Couvidat, 2011; Ulrich and Rhodes, 1977, and references therein). Solar oscillations, influenced by temperature, composition, and velocities, offer valuable information about conditions inside the sun. Therefore, accurately identifying and measuring these oscillation modes is crucial in helioseismology. The discovery of solar oscillations took place in 1962 when Leighton, Noyes, & Simon utilized Doppler shifts in solar disk velocity measurements (e.g., Evans and Michard, 1962; Leighton et al., 1962). They identified recurring patterns with a 5-minute cycle, labeling them as five-minute oscillations (e.g., Jensen and Orrall, 1963; Leighton et al., 1962). Initially, scientists were perplexed by the nature of these oscillations, leading to the exploration of various theories. Research conducted by Ulrich (1970) and Leibacher and Stein (1971) proposed that these oscillations are acoustic modes restricted within the sun's interior. Initially, the 5-minute vertical oscillations were perceived as chaotic and localized, with each region moving independently. However, they were recognized as pressure driven sound waves (or p-modes) originating from the convective zone. These oscillations are linked to turbulent convection motion within the sun. The solar interior hosts millions of resonant p-modes, causing surface vibrations lasting from minutes to hours (e.g., Bachmann and Brown, 1993; Fossat et al., 1987; García et al., 2001; Toutain and Froehlich, 1992).

As acoustic waves from the sun hit the photosphere and bounce back down, they agitate the gases, prompting them to rise and descend in a slow, rhythmic manner at 5-minute intervals. In Figure 1.2, the alternating patches denote gas movement downward (red)

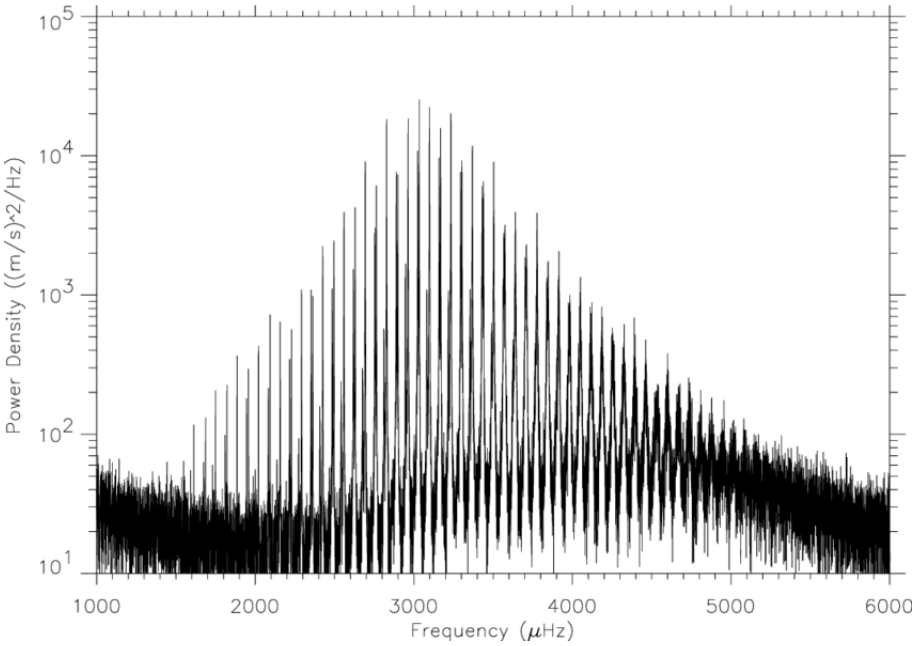

Figure 1.3: The acoustic p-mode spectrum of the sun, analyzed from the first eight months of Global Oscillations at Low Frequencies (GOLF) data, exhibiting a signal-to-noise ratio of 3000 at 3 mHz (Credit: M. Lazrek; F. Baudin and L. Bertello).

and upward (blue). Each 5-minute cycle represents the duration for localized motion to transition from outward movement to inward, and then back to outward again. Figure 1.3 displays a power spectrum of global solar oscillations which peaks at 3.3mHz (or $\approx$ 5 min) at the solar photosphere. These 5-minute oscillations or acoustic waves are confined within sun's interior and cannot travel to sun's atmosphere. These oscillations resonate within resonant cavities or spherical shells inside the sun, similar to echoes reverberating within a cave. Density and temperature gradients within the sun create a resonant cavity effect, causing sound waves to reflect or refract (see Figure 1.4). These waves follow specific paths, offering valuable insights into the sun's internal dynamics and structure. The sharp decrease in density at the solar surface results in sound waves with frequencies below approximately 5mHz (periods longer than 3.3 minutes) being reflected and trapped within the sun. Consequently, the sun resonates at discrete frequencies known as normal mode frequencies of pressure modes.

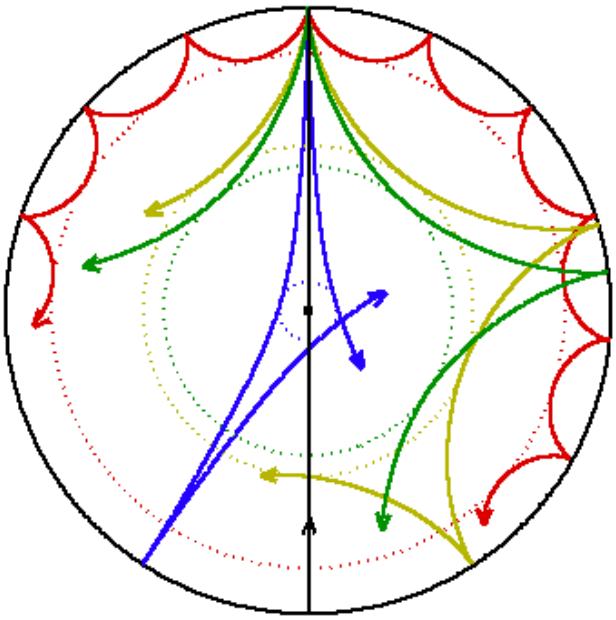

Figure 1.4: The diagram describes the paths of various acoustic waves travelling within the sun. Near the surface, acoustic waves reflect due to a significant decrease in density. Towards the bottom, the paths bend as the sound speed and temperature rise with the depth. The angle of reflection determines the depth of the penetration of acoustic waves. A shallower angle results in the shallower penetration (Credit: Jørgen Christensen-Dalsgaard).

In the sun, there are several million normal modes, each characterized by observed periods ranging from 3 to 12 minutes, typical surface velocities of about 5 cms^{-1}, and lifetimes lasting a few days. Similar to the energy states of the hydrogen atom, the individual normal modes of the sun are defined by three numbers: the spherical harmonic degree l, azimuthal order m, and the number of nodes in the radial direction n. A linear theory delineates these slight amplitude oscillations, with spherical harmonics identified by their degree and azimuthal order denoted by l and m correspondingly, thereby defining the angular aspect of the eigenfunctions of p-mode (cf., Figure 1.5). The most comprehensive representation of the velocity field related to these oscillations can be illustrated as follows (Demarque and Guenther, 1999):

$$v(r,\theta,\phi,t) = \sum v_{n,l}(r) Y_l^m(\theta\phi) e^{-i\omega_{nlm}t}, \tag{1.7}$$

The p-modes characterized by lower (higher) values of l delve more (less) deeply into the sun, thus exhibiting larger (smaller) inner turning radii. This characteristic renders them valuable for probing the solar interior Demarque and Guenther (1999).

1.1.2 The Solar magnetic field

The sun's magnetic field, crucial for governing dynamics across spatial and temporal scales, originates within its solar interior. Differential rotation between the sun's equator and poles drives the generation of this magnetic field, predominantly through a dynamo process operating at the solar tachocline, that serves as the interface between the radiative and convective zones. This dynamo theory explains how a fluid, which rotates, convects, and conducts electricity, can sustain a magnetic field by transforming kinetic energy into an electromagnetic energy (e.g., Choudhuri et al., 1995; Dikpati and Choudhuri, 1994; Hathaway et al., 2003; Parker, 1979; Priest, 2012; Schrijver et al., 2002). The plasma shearing at the tachocline due to differential rotation amplifies the magnetic field strength through

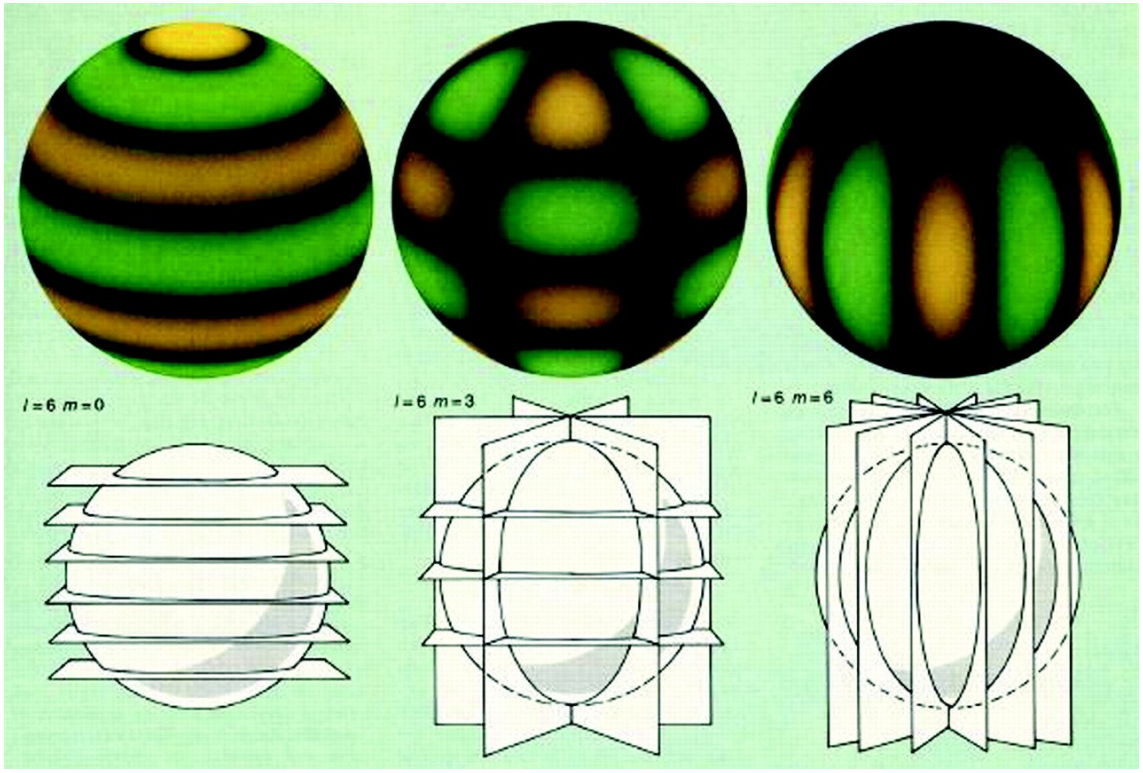

Figure 1.5: Moving towards low-degree harmonics: instances of $l = 6$ with various values of $m = (0, 3, 6)$, transitioning from polar mode to equatorial mode (Credit: J.W. Leibacher; P. Demarque and D. B. Guenther; Demarque and Guenther (1999)).

the Lenz law. Additionally, the convective motion and differential rotation contribute to generating electromagnetic energy, thus maintaining the sun as a self-sustaining dynamo. Numerous reviews have discussed the generation of the magnetic field (e.g., Hathaway et al., 2003; Ossendrijver, 2003), including considerations of magnetic field measurements and challenges in the solar atmosphere (e.g., Stenflo, 2013; Wiegelmann et al., 2014). The generated magnetic field connects the solar interior to the solar atmosphere, where shearing motion amplifies its strength, resulting in strong localized magnetic fields and associated fluxes at the surface of the photosphere. The sun's magnetism can broadly be classified into two categories, namely large-scale active regions and small-scale quiet-sun magnetic fields. The magnetic field is accurately measured on the sun's surface, called the photosphere. It has a big impact on different processes in the solar atmosphere. This magnetic field is important because it connects the sun's interior to its atmosphere and interplanatry space. It interacts with all encountered matter, influencing their dynamics through perturbation or confinement.

The magnetic field actively alters factors such as normal gas flows, convection patterns, and wave propagation at the solar surface and deeper, leading to the emergence of phenomena like sunspots and plages. In the solar atmosphere, the magnetic field exerts direct influence on the behavior of gas, exercising significant control over its dynamics, as evidenced by prominences, solar flares, and numerous dynamical plasma processes. The sun undergoes an 11-year activity cycle, characterized by the presence of sunspots on its surface. Strong localized magnetic fields are created by shearing plasma motion, leading to the formation of sunspots during solar maxima. This solar cycle influences magnetically driven phenomena such as coronal mass ejections, solar flares, and prominence eruptions. During solar maxima, the intensity of sunspots and other magnetic activities increases. The quiet-sun also exhibits an ambient magnetic field of approximately 5 Gauss. Solar radiation levels, solar material ejections, sunspot numbers, solar flares, and coronal

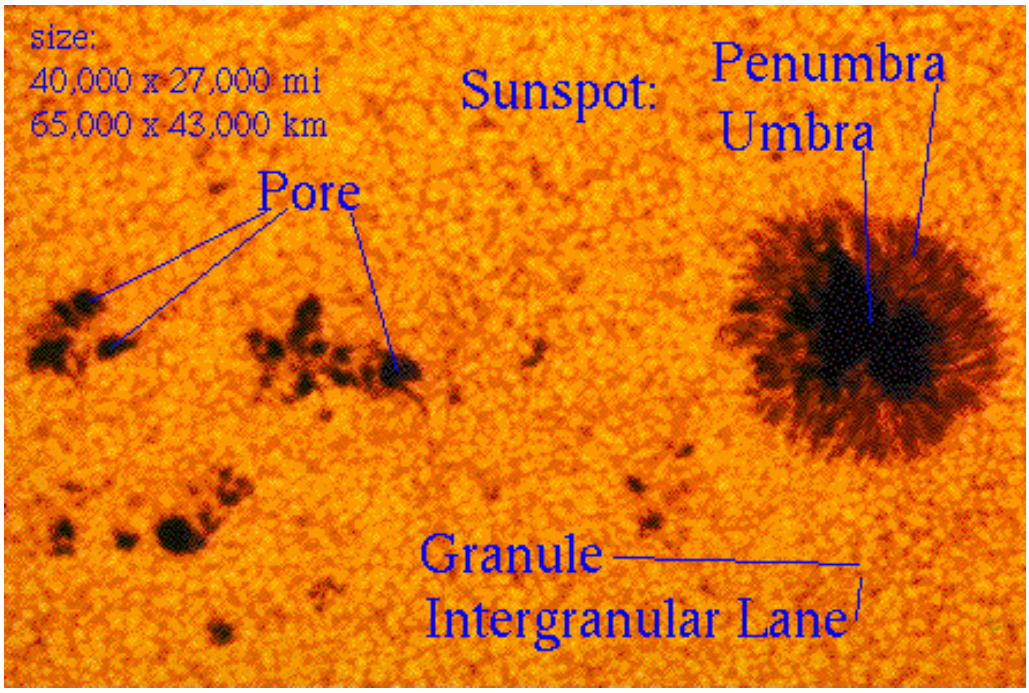

Figure 1.6: This image describes the magnified areas highlighting specific features of the strongly magnetized active region (AR) sunspot, pore, and the quiet-sun (QS) granules. (Credit: NASA).

loops all fluctuate synchronously, transitioning from active to quiet phases and back again, completing an 11-year solar cycle.

1.1.3 Exterior of the sun

The solar atmosphere consists of gas and plasma enveloping the outer layer of the sun, allowing photons to escape into space. The exterior of the sun is divided into four distinct regions, i.e., the photosphere, chromosphere, transition region, and corona, each encircling the sun in its unique way. When considering the sun on a larger scale, these layers are closely interconnected. Essentially, the solar atmosphere is what we directly observe on the sun's surface. Defining its upper boundary poses a challenge as it merges with the solar wind, which is sometimes regarded a part of the solar atmosphere. In the following section, a brief overview of these layers will be provided.

Photosphere

The photosphere, acts as the visible outer layer of the sun, stretches across several hundred kilometers and emits most of the sun's visible light as a black body. It maintains temperatures ranging from 6000 to 4000 Kelvin, with an average temperature hovering around 5800 Kelvin (e.g., Foukal, 2008). Additionally, it has an average density of $3{\times}10^{-7}$ grams cm^{-3}. This density attribute leads to a pressure scale height of approximately 100 kilometers, indicating a state of near hydrostatic equilibrium. Consequently, the gas is swiftly transformed to an opaque state, constraining the overall vertical expansion of the photosphere to roughly 500 kilometers, a mere fraction of the solar radius, amounting to less than 0.1%. This layer showcases various features like granulation, supergranulation, and pores (cf., Figure 1.6) (e.g., Nordlund et al., 2009; Stein, 2012). Granules, cellular features averaging about 1000 km in size and lasting roughly 10–20 minutes, cover nearly the entire solar surface, with millions existing at any given moment. Each granule features a central bright region representing upward-moving plasma with a velocity ranging from 0.5-1.5 km s^{-1}, exhibiting horizontal motion before cooling and descending through darker intergranular lanes (e.g., Bello González et al., 2009). The average lifespan of granules falls between 5 and 10 minutes. Doppler measurements reveal giant cells, known as supergranular cells, with typical sizes of 20-70 Mm, where plasma ascends at the center with a speed of 30 m s^{-1} before moving outward horizontally at 350 m s^{-1} and descending through the cell boundaries (e.g., Hathaway et al., 2002). These cells endure for 1–2 days on average.

Besides, the photosphere displays sunspots as prominent features, constituting about 5% of the sun's surface. Sunspots consist of central umbral regions, with predominantly vertical magnetic fields, and surrounding penumbral regions, featuring inclined magnetic fields. These regions, substantially cooler than the ambient photosphere at around 4000 K, have distinct characteristics, including the umbra with magnetic field magnitudes ranging

from 1000 to 3000 G, and the penumbra with strengths of approximately 100–300 G (e.g. Priest, 2014, 2012). Sunspots typically range from 5 to 25 Mm in size and last for hours to days during their appearance on the photosphere. They vary over an 11-year cycle, shifting in location and appearing in groups across ± 40 degree altitude from the equator. These cycles, depicted in the Maunder butterfly diagram (cf., Figure 1.7), have been extensively studied. The photosphere reveals a multitude of magnetic structures and physical phenomena. Acting as the sun's lowest directly observable layer, it serves as a gateway to the solar interior through helioseismology. Figuring out how the photosphere works is really important for understanding many things about the sun and other stars.

Chromosphere

Above the photosphere, the chromosphere extends with a thickness varying between approximately 1 to 2 Mm. On average, it is around 1500 km thick. In this layer, the temperature gradually rises to about 10,000 K, while the density sharply drops compared to the photosphere, by a factor of 10^{-4} (e.g., Bray and Loughhead, 1974). In the event of total solar eclipses, the chromosphere displays vivid colors, showcasing varying shades of pink owing to the prevalence of three notable emission lines (violet, blue, and red) found within hydrogen Balmer Hα 6563 Å emissions (cf., 1.8). The chromosphere is observable across various wavelengths, including far UV, millimeter wavelengths, and within the cores of strong spectral lines such as Mg II h 2796 Å & k 2803 Å, He I 10830 Å, C II 1334 Å/1335 Å, Ca II H 3968 Å & K 3933 Å, and Hα 6562 Å(e.g., Beckers and Tallant, 1969; Bjørgen et al., 2018; Hansteen et al., 2023; Kayshap et al., 2018c; Kerr et al., 2015; Kianfar et al., 2020; Leenaarts et al., 2016; Lites and Skumanich, 1982). Studying the chromosphere is crucial because it may be the source of all nonthermal energy and mass supply that eventually goes to the corona and forms the solar wind (e.g., Carlsson et al., 2019; Schwenn, 2006; Temmer, 2021). Theoretical studies emphasize

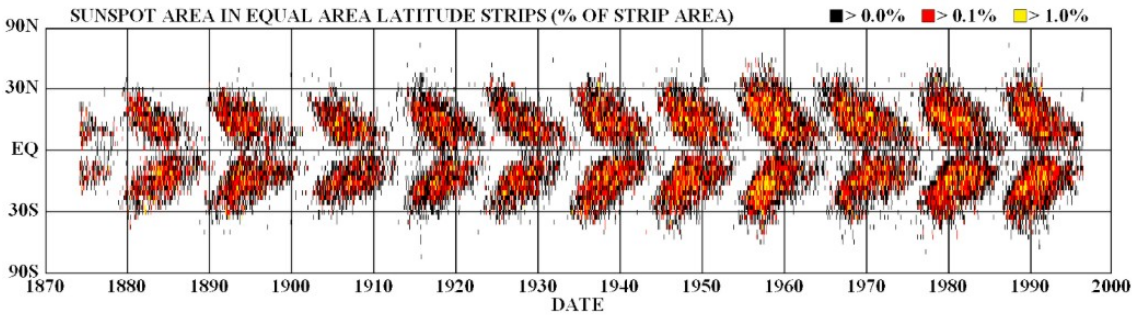

Figure 1.7: The provided graph illustrates the distribution of sunspots from 1870 to 1995. Notably, the central line, extending horizontally from left to right, denotes the sun's equator, with sunspots occurring both north and south, positioned above and below this reference line (Credit: NASA's Marshall Space Flight Center / D.H. Hathaway).

how important the chromosphere is as it shifts from LTE to non-LTE, from high to low plasma , and from single- to multi-fluid MHD (Avrett and Loeser, 2008; Carlsson and Stein, 1992). This complexity poses challenges in interpreting observations and requires intensive computational modeling (Carlsson et al., 2019). While granular convection governs small-scale dynamics in the photosphere, the chromosphere is mainly influenced by waves, notably acoustic waves with a three-minute period in internetwork regions (McAteer et al., 2004). Additionally, there is growing evidence indicating that MHD waves exist in the magnetic structures forming the chromospheric (e.g., Bogdan et al., 2003; Jess et al., 2023, and references therein).

Transition Region

Above the chromosphere there is a thin region known as the solar transition region where the temperature increases sharply to over a million Kelvin and density decreases abruptly (Gabriel, 1976; Mariska, 1992). At such high temperatures, hydrogen becomes ionized, meaning it loses its electron and becomes challenging to detect. Instead of hydrogen, the transition region primarily emits radiation from ions like C IV, O IV, and Si IV. These ions emit ultraviolet light, which can only be observed from the space. The transition region serves as the site where plasma undergoes rapid heating (or cooling) to (or from)

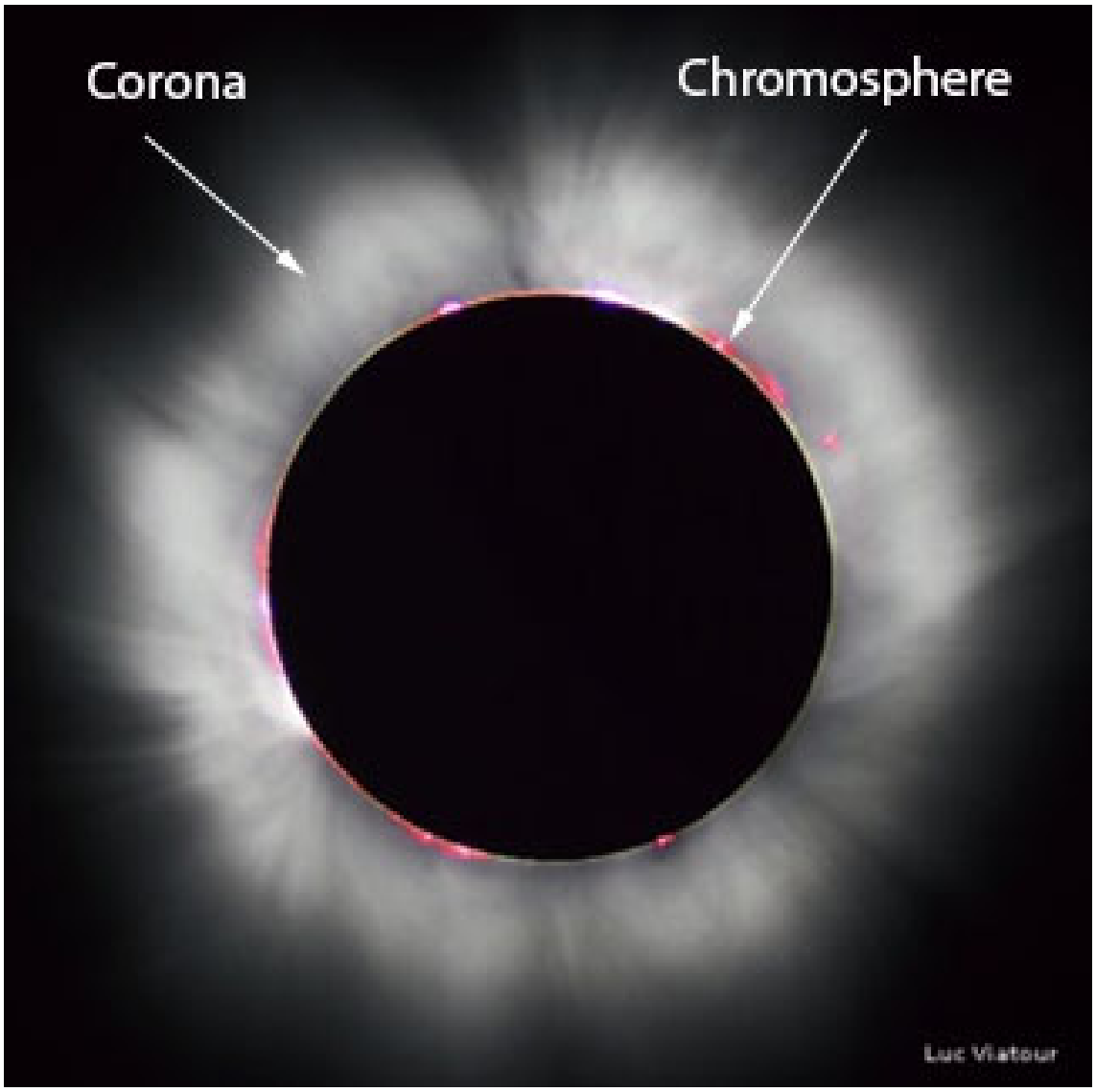

Figure 1.8: The image is captured during the 1999 solar eclipse showing both the chromosphere and the corona of the sun (Credit: Luc Viatour).

coronal temperatures within a very short vertical range (approximately 100 km), and it is detectable at UV and centimeter wavelengths. The average altitude of the transition region varies across different solar regions. For example, in the quiet sun, it may be around 1700±800 km at temperatures of 10^5 K, while in coronal holes, it may extend much higher, ranging between 1500 to 15,000 km (e.g., Priest, 2014). This layer acts as a crucial link between the cooler chromosphere and the hotter corona. Various dynamic plasma and wave processes originating in the chromosphere encounter the transition region before they reach the corona. Processes such as coronal thermal conduction, plasma condensation, backward-moving plasma in localized magnetic domains, and oscillatory motions that couple the lower atmosphere to the corona may also be influenced by the solar transition region. These dynamic phenomena encounter several discontinuities at the transition region, including local characteristic speeds, plasma, and magnetic field properties, which affect their dynamics and energetics. Hence, the transition region significantly influences the transport of mass and energy between the chromosphere and corona, regulating emissions, flows, and temperatures.

Corona

The corona is the outermost atmospheric layer of the sun. It can be observed with the naked eye during the total eclipse, appearing as a diffuse structure extending outward, as displayed in Figure 1.8. The configuration of the corona is largely influenced by the solar magnetic field. Free electrons in the corona trace the magnetic field lines, creating various structures like helmet streamers, visible as elongated, spiked cones during the solar eclipse. The solar corona exhibits very low resistivity, leading to a "frozen-flux condition" where the magnetic flux within a fluid element remains constant over time. Observations of spectral lines in the corona reveal the presence of highly ionized ions like Fe X, Fe XI, and Fe XI (e.g., Harrison et al., 1995, 1997; Mason et al., 1997), indicating temperatures

of at least 10^6 K. At such high temperatures, hydrogen and helium, along with other minor elements like oxygen, nitrogen, and carbon, are deprived of their electrons, while heavier trace elements like calcium and iron preserve some electrons in the presence of intense heat. Advancements in instrumentation have enabled observations of the corona even without the occurrence of a total solar eclipse, as illustrated in Fig. 1.10 (panel d). The corona's temperature, ranging from a million Kelvin to 10 MK, adds to its intrigue. The unusually high temperature of the corona remains a significant puzzle in solar physics, known as the Coronal Heating problem. Moreover, the corona's dynamical nature is strongly influenced by the ever-changing magnetic topology. The morphology of coronal structures is intricately linked to the strength and topology of the magnetic field, dictating the dynamics of the corona. Consequently, the radiation characteristics from the corona are closely intertwined with the underlying magnetic field structure, and frozen in plasma.

1.2 Variation of the Density and Temperature

As we ascend to the top of the solar photosphere, the temperature gradually decreases to its lowest point. This temperature decline in the photosphere happens because of radiative equilibrium, which necessitates a negative temperature gradient for efficient radiative energy transport through this layer. However, as we move upward through the chromosphere, the temperature begins to rise, exceeding its minimum value. Contrary to the behavior in the photosphere, this temperature increase in the chromosphere, reaching around 20,000 K, does not adhere to radiative equilibrium principles. This discrepancy is likely due to non-radiative heating processes within the quiet-sun regions of the solar chromosphere, such as acoustic waves or reconnection events. Consequently, the average temperature rises significantly beyond the minimum temperature level. Within the lower chromosphere, hydrogen undergoes ionization, absorbing energy and enhancing its heat-retaining capacity, thereby establishing a temperature plateau. At heights beyond 2.0 Mm,

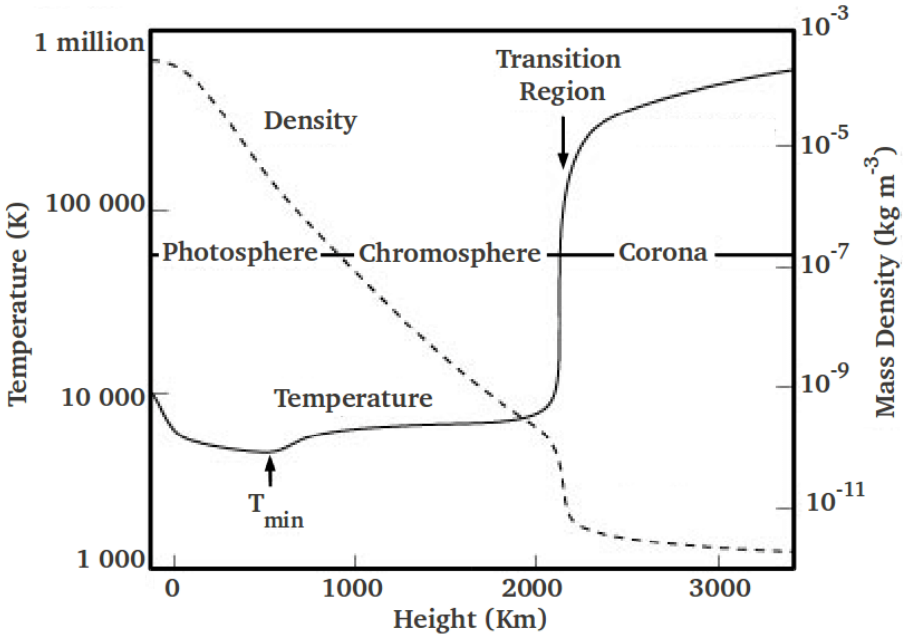

Figure 1.9: The variation in temperature and density as we move upward in the solar atmosphere derive from the VAL model (Credit: Eugene Avrett/ (Priest, 2014)).

the neutral hydrogen density is too low to completely absorb the energy produced by acoustic or shock waves. As a result, a notable amount of this energy is conveyed to the upper chromosphere and the transition region (TR) from the solar corona through thermal conduction. This leads to a sudden temperature spike, surpassing 10,000 K, causing the upper chromosphere to become transparent to Hα emissions, which aids in its cooling and forms a secondary temperature plateau ranging between 20,000 K and 30,000 K. Within the transition region (TR), the temperature experiences a sharp increase, averaging at 1.0 MK in the inner corona. While the density is highest at the solar photosphere, it undergoes a steep decline in the transition region and the inner corona (refer to Figure 1.9).

As one moves away from the solar core, it's reasonable to anticipate a gradual decline in temperature, adhering to the expected thermal gradient. However, the rise of temperature beyond the temperature minimum, indicating the presence of additional heating mechanisms beyond standard radiative energy transfer. Despite extensive studies, a widely

accepted model to explain this phenomenon is still lacking, as traditional radiative transfer models fail to fully explain the observed temperatures. Two primary theories have been proposed to account for the heating of the chromosphere and corona: (i) Magnetic reconnection, a process in which magnetic field lines of opposite orientation convert magnetic energy into thermal energy; and (ii) Wave propagation, specifically acoustic and magnetoacoustic waves generated by movements in the upper convection zone. These waves dissipate energy as atmospheric properties change vertically in a stratified medium. My thesis delves into the dynamics of waves in the solar atmosphere. In the upcoming section, I will a brief introduction to waves in solar atmospheres is provided.

1.3 The Sun at Different Wavelength

Studying the sun across different wavelengths allows us to see it at different layers (or different heights) and temperatures. Reseachers use a range of instruments, each tuned to a specific wavelength, to explore mysteries surrounding our nearest star. For example, the photosphere, acting like a blackbody, is visible in visible light, the chromosphere can be seen both in visible wavelength (Ca II and Hα) as well as in UV wavelength. Transition region and corona can be seen in ultraviolet (UV) and extreme ultraviolet (EUV) channels. The hottest parts of the corona even emit X-rays. When the solar corona is captured in the EUV at 1 million Kelvin, it unveils a variety of structures magnetically linked to cooler regions below—the chromosphere and the photosphere (cf, Figure 1.10). Our understanding of the sun's atmosphere primarily comes from studying the light it emits. Comparing images taken at different wavelengths gives us important insights into the structure of its layers. Advances in solar observations have allowed us to directly examine the emergence and vanishing of solar magnetic fields, along with their interactions with solar plasma. It is now acknowledged that magnetic fields originating in the photosphere

and produced in the convection zone control the behavior of the chromosphere, transition region, and corona.. Magnetic field concentrations at the photosphere often correspond to intense brightenings across various imaging bands, from UV to X-ray. These observations are continually expanding our understanding of magnetic field coupling throughout the solar atmosphere.

1.4 Magnetohydrodynamic Waves in the Solar Atmosphere

Recent observations from both space and ground-based instruments have verified the ubiquitous existence of waves within different magnetic structures of the solar atmosphere. Understanding the generation, drivers, physical properties, and dissipation mechanisms of these waves in the localized solar atmosphere is crucial for comprehending their potential contributions to chromospheric and coronal heating, as well as constraining plasma dynamics and flows. Solar oscillations are typically represented by temporal changes in observable values. The easiest way to detect these oscillations is through intensity variations, which exhibit regular periods of increasing and decreasing intensity. However, intensity variations can be influenced by changes in density, temperature, or line-of-sight motions. On the other hand, Doppler velocity, offers a more fundamental observable quantity describing the medium, showing blueshifts and redshifts. Since 1960s, it has been known that patches of the sun's surface oscillate with a period of about five minutes (e.g., Leighton et al., 1962), initially attributed to local convective motions but later recognized as the superposition of many global resonant modes of oscillation (e.g., Deubner, 1975; Stein and Nordlund, 2001; Ulrich, 1970). The sun supports various wave motions, predominantly acoustic and gravity waves, which establish global resonant modes. Although acoustic modes are the primary oscillations in the sun, their propagation is affected by factors such as gravity, internal stratification, bulk motions, and magnetic fields. The frequencies and characteristics of these oscillations provide valuable information about

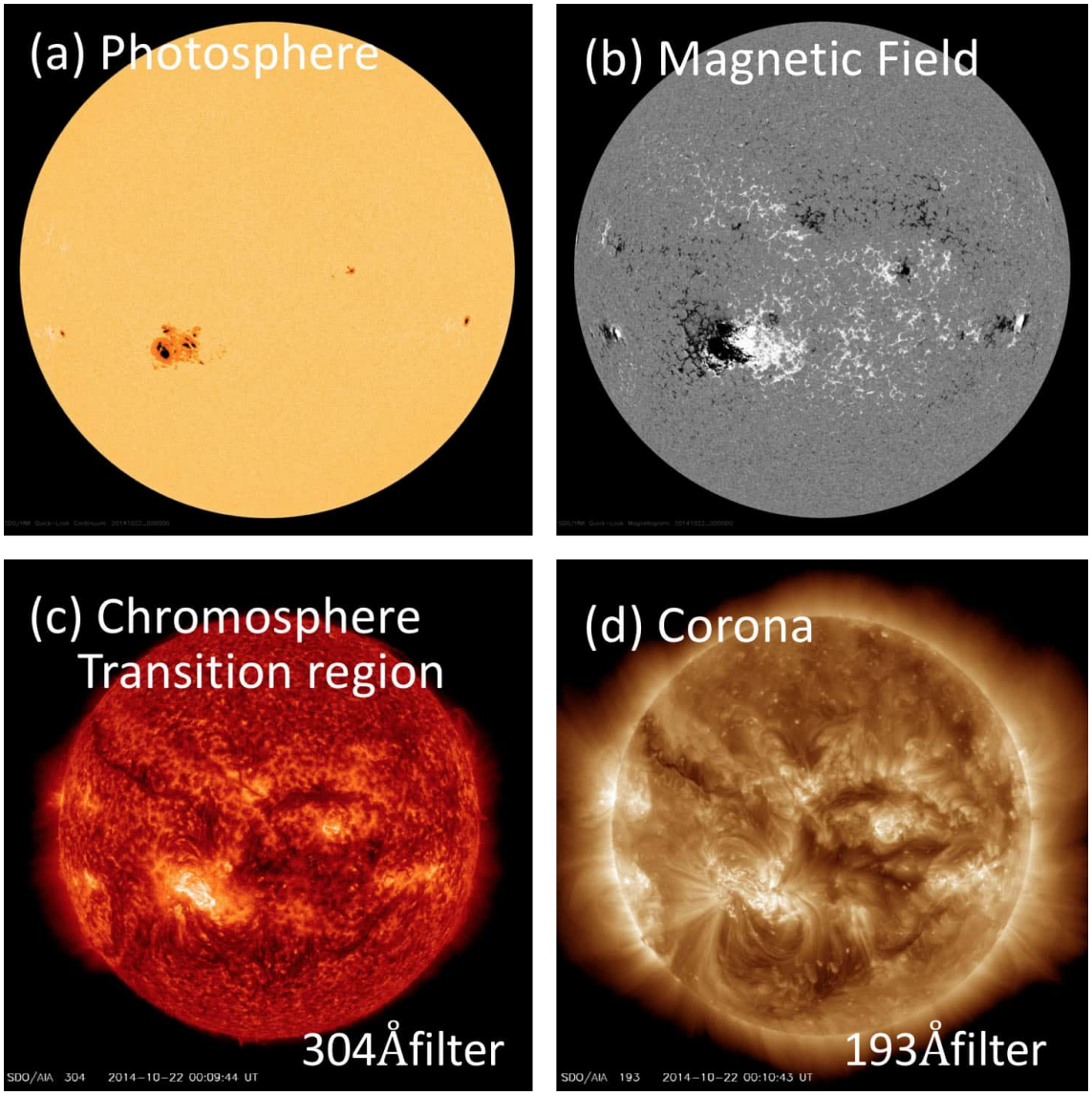

Figure 1.10: Observations of the sun across multiple wavelengths, captured by the AIA & HMI onboard the SDO satellite. (Credit: SDO/AIA, HMI).

the physical condition of solar interior. The p-modes represent intrinsic global acoustic oscillations within sub-photospheric layers, reaching the surface photosphere where 5.0-minute oscillations hold significant influence. These p-modes have a potential to leak and propagate upwards within the magnetic solar atmosphere, potentially playing a role in its heating if their frequency surpasses the local acoustic cut-off frequency. Typically, the solar chromosphere has an acoustic cutoff frequency of approximately 5 mHz, which theoretically prevents acoustic waves from propagating upward in the solar atmosphere below this frequency. However, due to the chromosphere's magnetic properties, waves may propagate as magnetoacoustic waves. The strong magnetic field alters the acoustic cutoff effect, potentially allowing wave propagation if $\omega > \omega_c \cos\theta$, where θ represents the magnetic field's inclination angle from the vertical direction (e.g., De Pontieu et al., 2004; Jess et al., 2013; McIntosh and Jefferies, 2006).

1.4.1 The influence of magnetic fields

The significance of the magnetic field within a region can be measured using the plasma beta, denoted as , which represents the ratio of plasma pressure to magnetic pressure. It is defined as follows:

$$\beta = \frac{8\pi p_{gas}}{B^2} \tag{1.8}$$

When plasma $\beta \gg 1$, plasma pressure holds significance, whereas in the case of plasma $\beta \ll 1$, magnetic fields exert dominance in the medium. Determining the precise value of plasma through observations proves challenging. However, it is postulated that the $\beta = 1$ layer resides near the sunspot photosphere, dividing the medium into regions of high β plasma ($\beta \gg 1$) below, and low β plasma ($\beta \ll 1$) above (e.g., Mathew et al., 2004). The sun, made up of compressible plasma, generates magnetoacoustic and Alfvén waves observed throughout its interior and atmosphere. Complexity arises in the wave behavior within the

sun due to plasma structuring influenced by robust magnetic fields, density stratification, and varying temperatures. In the absence of magnetic fields ($\beta \gg 1$), only sound waves can propagate within the medium. The restoring force for sound waves is the pressure gradient force. In an ideal gas, a sound wave induces compressions and rarefactions that propagate isotropically at the sound speed, denoted as c_s, and given by the formula:

$$c_s = \sqrt{\frac{\gamma p_o}{\rho_0}} \tag{1.9}$$

A sound wave typically involves perturbations in velocity, density, and pressure. However, in a conducting plasma like the corona, oscillations result in both magnetic and associated perturbations, transforming them from sound waves to magnetic disturbances. The magnetic field induces anisotropic wave propagation, leading to variations in propagation speeds. When magnetic fields are perturbed, they encounter either magnetic tension or magnetic pressure forces as restoring forces. In the ideal magnetohydrodynamic (MHD) model of a uniform plasma, three types of waves emerge, namely, Alfvén waves, slow magnetoacoustic waves, and fast magnetoacoustic waves. These waves display varying characteristics based on the orientation of the wave vector concerning the magnetic field. Typically, the propagation speeds of these waves are ordered from slower to faster: slow magnetoacoustic, Alfvén, and fast magnetoacoustic waves.

The Alfvén Waves

The wave is a transverse wave that is incompressible and travels along magnetic field lines within the solar corona. Alfvén waves occur when the magnetic tension force serves as the sole restoring force. The speed at which Alfvén waves propagate is determined by

$$v_A = \frac{B}{\sqrt{\mu_o \rho}} \tag{1.10}$$

In the equation, v_A represents the Alfvén speed, B denotes the background magnetic field, and ρ stands for the background density of the large-scale homogeneous atmosphere. Alfvén waves cannot be detected using only imaging instruments because they don't cause shifts in the axis of the magnetic structure or changes in density and intensity. Therefore, in theory, intensity observations alone cannot detect Alfvén waves.

Fast magnetoacoustic waves

Compressible waves are generated if both magnetic force and pressure gradient act as the restoring force. If the magnetic force and pressure gradient align in phase, these compressible waves evolve into fast magnetoacoustic waves. The phase speed of these fast waves is determined by (Priest, 2014)

$$\frac{\omega}{k} = \left(\frac{1}{2}(c_s^2 + v_A^2) + \frac{1}{2}\sqrt{(c_s^2 + v_A^2)^2 - 4c_s^2 v_s^2 cos^2\theta}\right)^{1/2} \tag{1.11}$$

When plasma β is considerably less than one, isotropic propagation of fast waves occurs at the speed of v_A. Conversely, when plasma β greatly exceeds unity, isotropic propagation of fast waves occurs at the speed of c_s, resembling the behavior of acoustic waves.

Slow magnetoacoustic waves

Slow magnetoacoustic waves manifest when the pressure gradient force and the magnetic force are out of sync, mirroring the conditions for generating fast waves. The phase speed of these slow waves is delineated as (Priest, 2014)

$$\frac{\omega}{k} = \left(\frac{1}{2}(c_s^2 + v_A^2) - \frac{1}{2}\sqrt{(c_s^2 + v_A^2)^2 - 4c_s^2 v_s^2 cos^2\theta}\right)^{1/2} \tag{1.12}$$

Unlike the fast waves, the slow waves propagate predominantly along magnetic field lines ($\theta = 0$) and cannot travel across them ($\theta = \pm\pi/2$). They exhibit characteristics akin to

sound waves in the low plasma β regime, behaving as longitudinal waves along magnetic field lines at the speed of c_s.

1.4.2 Propagating waves in the solar atmosphere

The p-modes are typically predominantly acoustic waves because of the high plasma beta ($\beta \sim 10^2$). As the balance of forces changes with altitude, moving from a region dominated by gas pressure beneath the photosphere to a domain dominated by magnetism in the corona, the nature of the waves experiences alteration, resulting in mode transformation. In the upper atmosphere, under the influence of strong magnetic field these p-modes will be converted magnetoacoustic oscillations (e.g., Bloomfield et al., 2006; Khomenko and Calvo Santamaria, 2013; Kostik and Khomenko, 2013) and these oscillations could potentially contribute to the heating of the chromosphere and corona. But the wave propgation from the phtosphere to chromosphere, transition region, and corona depends on the acoustic cut-off freuency. Acoustic cutoff frequency, ω_c, that, for an isothermal atmosphere, is expressed as (Lamb, 1909):

$$\omega_c = \frac{\gamma g}{2c_s} \tag{1.13}$$

ω_c is the cut-off frequency, g is the gravitational acceleration of the sun, γ is the adiabatic constant, and c_s is the isothermal sound speed. Waves with frequencies above the cut-off frequency are capable of propagating into the upper atmosphere, whereas those with frequencies below the cut-off frequency do not propagate into the upper atmosphere. Nevertheless, waves having frequency below the acoustic cut-off can propagate into the solar atmosphere and can contribute to the atmosphereic heating (e.g., Beck et al., 2009; Jess et al., 2009; Ulmschneider, 1971). In the presence of strong magnetic field, oscillations having frequency less than acoustic cut-off frequency has been reported in the chromosphere (e.g., Bocchialini et al., 1994; Kontogiannis et al., 2010b; Vecchio et al.,

2007). It is suggested that in the presence of strong magnetic field, radiative relaxations time gets changed and it leads to decreament in the cut-off frequency (e.g., Khomenko et al., 2008; Roberts, 1983). Consequently, inclined field also decrease the cut-off frequency (e.g., de Wijn et al., 2009; Heggland et al., 2011; Jess et al., 2013; Kontogiannis et al., 2014). The inclined magnetic field alters the acoustic cut-off effect and allowing wave propagation if $\omega > \omega_c \cos\theta$, where θ represents the magnetic field's inclination angle from the vertical direction (e.g., De Pontieu et al., 2004; de Wijn et al., 2009; Jess et al., 2013; McIntosh and Jefferies, 2006). The power correspond to low frequency waves along with the power from high frequency waves might boost the energy flux supply, which could be crucial in regions with strong magnetic fields where convective motions are limited.

Magnetoacoustic waves exhibit mode conversion, which takes place at the equipartition layer as shown in Figure 1.11. This layer is where the sound speed equals the Alfvén speed ($c_s = v_A$), facilitating energy transfer within the waves (e.g., Cally, 2005). It is closely associated with the $\beta = 1$ layer, plasma pressure equals magnetic pressure. Initially, at this level, either conversion or transmission may occur. During conversion, the fats magnetoacoustic wave convert into fast magnetic wave at $c_s = v_A$ layer as shown in Figure 1.11. During transmission, the fast magnetoacoustic wave is transformed to a slow magnetoacoustic wave (e.g., Stangalini et al., 2011). The choice between transmission and conversion relies on the angle between wave vector and the magnetic field. It favors transmission when the angles are small and conversion when they are higher (e.g., Schunker and Cally, 2006). There is a possibility of the fast magnetic wave converting into the Alfvén wave later on, typically happening close to the inflection point of the curve depicted in Figure 1.11. At the edge of the transition region, where the Alfvén speed gradient undergoes a sharp change, the fast-mode wave reflects. It could potentially undergo conversion once more as it descends through the equipartition layer.

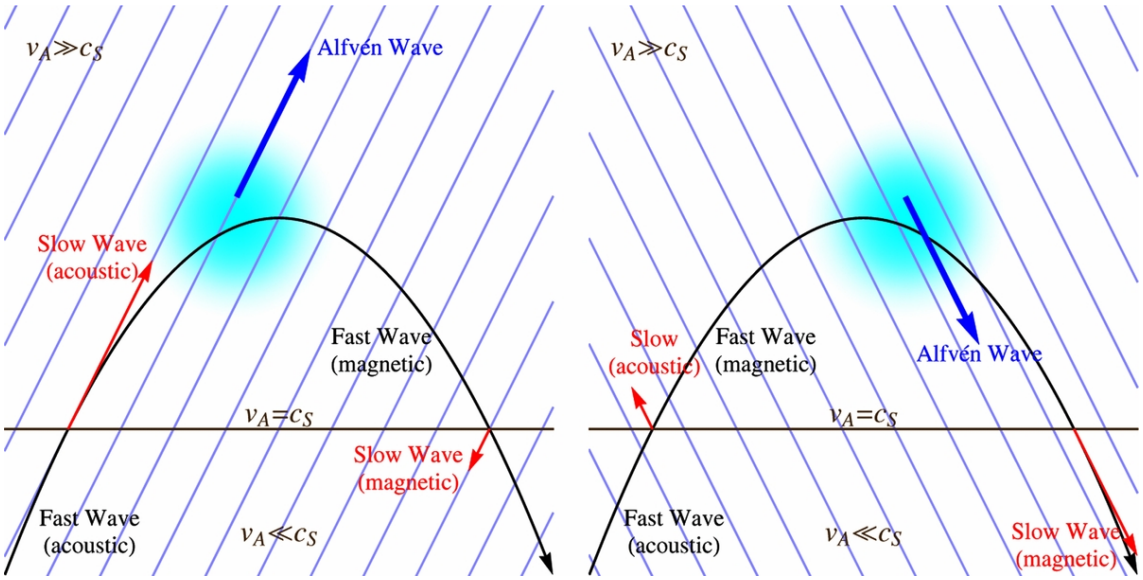

Figure 1.11: Propagation of waves and mode conversion in the stratified atmosphere. In both panels, the blue diagonal lines illustrate the orientation of the background magnetic field. The arrowed lines represent the wave vectors (Credit: Khomenko and Cally (2012))

Observations of waves in the quiet-sun

Observations in quiet solar regions have provided valuable insights into the behavior of waves. Through multi-spectral line multi-height observations, researchers have highlighted the impact of the magnetic field on wave propagation in various solar regions, including plage, sunspot, network regions, and the quiet-sun. Unlike in sunspots, where the magnetic field tends to be stronger and more organized, it is generally weaker and less structured in quiet regions, posing challenges for the measurement. Magnetic elements within the quiet sun exhibit complexity and dynamism, with weaker inter-network magnetic elements demonstrating movement, merging, and cancellation, while stronger network elements display more organization. Recent studies have utilized spectropolarimetric observations to reveal the structures of network tubes, including their canopies, which differ from theoretical models, displaying dynamic and asymmetric forms (e.g., Kontogiannis et al., 2011). In localized regions, acoustic p-modes and convective motions instigate wave propagation within magnetic concentrations across the quiet-sun. The inter-network region

are dominated be 3 min periodicity. They appear as intermittent bright grains in Ca II H2V and K2V emissions, identified as acoustic shocks (e.g., Mathur et al., 2022; Vecchio et al., 2009). Whereas the network region are dominated by 5 min periodicity.

Essentially, these long-period oscillations create enhancements on power maps, known as power halos, as they propagate to the chromosphere. These halos are most noticeable in the photosphere and coincide with chromospheric magnetic shadows for 3-minute waves (e.g., Jain and Haber, 2002; Krishna Prasad et al., 2016; Stangalini et al., 2012). The distinct power distribution in halos/shadows corresponds to the height of the magnetic canopy, where plasma $\beta = 1$. In the vicinity of network elements with low-lying canopies, chromospheric power of short-period waves is suppressed, while photospheric power of long-period waves is amplified. These enhancements are significant for more inclined canopy fields, suggesting more efficient mode conversion (e.g., Hanson et al., 2015; Kontogiannis et al., 2010a). Table 1.2 provides a summary of the oscillations observed in the quiet sun.

Table 1.2: Periods of Network and Inter-network Oscillations (Credit: Khomenko and Calvo Santamaria 2013)

	Centers of mag. elements	Close surroundings	Inter-network beyond mag. elements
Photosphere	5 min	5 min	5 min
Chromosphere	Possibly 5 min	5 min enhanced 3 min shadowed	3 min shocks
Propagation	Up & down	Up & down	Up

Observations of waves in the sunspot

Sunspot oscillations have undergone extensive examination over numerous years (e.g., Beckers and Tallant, 1969; Bogdan, 2000; Bogdan and Judge, 2006; Brynildsen et al., 1999; Felipe et al., 2010b; Gurman et al., 1982; Khomenko and Collados, 2015). These solar features exhibit oscillations in both velocity (measured by Doppler shifts) and

intensity (representing thermodynamic quantity density) (cf, Figure 1.12). Analysis of time-seriesdata often uncovers distinct power peaks concentrated within period bands spanning 2 to 3 minutes, 5 minutes, and extending beyond approximately 20 minutes, with origins likely stemming from various physical mechanisms (e.g., Brynildsen et al., 2004; Felipe, 2019; Horn et al., 1997; Lites, 1992; Stangalini et al., 2012; Staude, 1999). The strong magnetic field found within sunspots, combined with its confined spatial distribution, significantly impacts the oscillatory behavior of the solar atmosphere. This interaction gives rise to oscillation modes that are absent in the quiet-sun and significantly alters the characteristics of the 5 minute oscillations. As per Bel and Leroy (1977), low-frequency waves could travel to the higher regions of the solar atmosphere through magnetic conduits such as sunspots and pores. Particularly, owing to the inclined magnetic fields, 5 minute oscillations may appear in different magnetic structures like spicules loops of active regions (e.g., De Moortel et al., 2002; De Pontieu et al., 2005, 2004). In sunspot umbrae, two main types of characteristic oscillations are observed. The first type, with periods of approximately 5 minutes, represents the response of the sunspot's magnetic flux tube to the 5-minute p-mode oscillations in the neighboring convection zone (e.g., Thomas, 1981; Thomas et al., 1982). The second type, with periods of around 3 minutes, consists of resonant modes specific to the sunspot's own oscillation (Thomas and Scheuer, 1982). Presently, there are two main theoretical frameworks explaining the 3-minute oscillations observed in sunspot umbrae. One model suggests that these oscillations are linked to a resonant mode of fast magneto-atmospheric waves, primarily confined within the photosphere and subphotosphere. These waves are triggered by unstable convection processes in the subphotosphere (e.g., Thomas and Scheuer, 1982). The other model proposes that these oscillations stem from a resonant mode of slow magnetoacoustic waves, mainly confined within the chromosphere. These waves are induced by broad-band acoustic input originating from the convection zone (Zhugzhda et al., 1987). These two

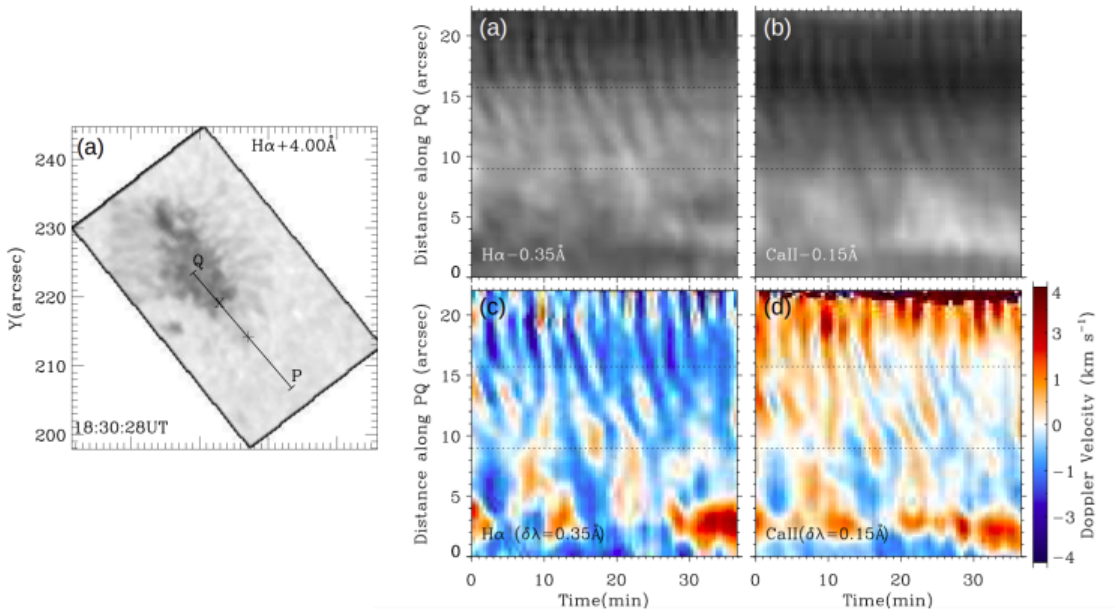

Figure 1.12: The left panel exhibits a raster image captured at a wavelength of $H\alpha$+4.0 Å of the active region. On the right panel, the time-distance maps are presented, depicting intensity (top row) and Doppler velocity (bottom row) for $H\alpha$ (left column) and $CaII$ (right column). The dashed horizontal lines mark the boundaries between the umbra and the penumbra (Credit: Ajor Maurya et al. (2013)).

models are commonly referred to as the photospheric resonance and the chromospheric resonance, respectively. These theoretical models are not mutually exclusive, and in fact, it is probable that both resonances occur in sunspot umbra.

1.5 Quasi-Periodic Pulsations in the Solar Atmosphere

Apart from the waves originating and coupling various layers of the solar atmosphere, corona is a hub for sudden releases of energy, like various types of jets, flares, and coronal mass ejections (CMEs). Oscillations, along with magnetohydrodynamic (MHD)

waves, are prevalent throughout the solar corona and are crucial for heating the coronal plasma (e.g., Erdélyi and Ballai, 2007; Nakariakov and Verwichte, 2005). Emissions from solar and stellar flares often exhibit quasi-periodic variations known as quasiperiodic pulsations (QPPs) (e.g., Parks and Winckler, 1969). In a standard occurrence, QPPs appear as recurring peaks on the light curve, each maintaining a consistent lifespan, thereby generating regular intervals between them (cf, Figure 1.13). Consequently, QPPs are characterized by their repetitive or periodic nature. They span a broad spectrum of periods ranging from fractions of a second to several minutes (e.g., Inglis and Nakariakov, 2009; Kislyakov et al., 2006; Kupriyanova et al., 2020; Nakariakov and Melnikov, 2009; Nakariakov et al., 2018; Van Doorsselaere et al., 2016; Zimovets et al., 2021, and references therin). Various periods of QPPs may correspond to different physical phenomena within the solar atmosphere. QPPs are most observable in emissions linked to flare-accelerated non-thermal electrons across hard X-ray, microwave, and white light frequencies. These pulsations occur throughout all phases of the flare, from pre-flaring to decay, and are often observed simultaneously across different bands, such as hard X-ray and microwave emission (e.g., Asai et al., 2001; Nakariakov et al., 2010a). The observed characteristics of QPPs (such as their periods, modulation, typical signatures, and spatial information) are linked to the physical properties of the flaring plasma. These characteristics can serve as diagnostic tools through the method of coronal seismology.

The mechanisms underlying QPPs are currently under intense investigation, with a general agreement suggesting their association with repetitive patterns of charged particle acceleration during magnetic reconnection, and/or periodic adjustments in accelerated particle dynamics. The periodicity can arise spontaneously or be triggered by magnetohydrodynamic (MHD) waves (e.g., McLaughlin et al., 2018). Specifically, the modulation of nonthermal charged particle dynamics by an MHD oscillation, such as the sausage mode, may contribute to the periodic nature (e.g., Zajtsev and Stepanov, 1982). Despite

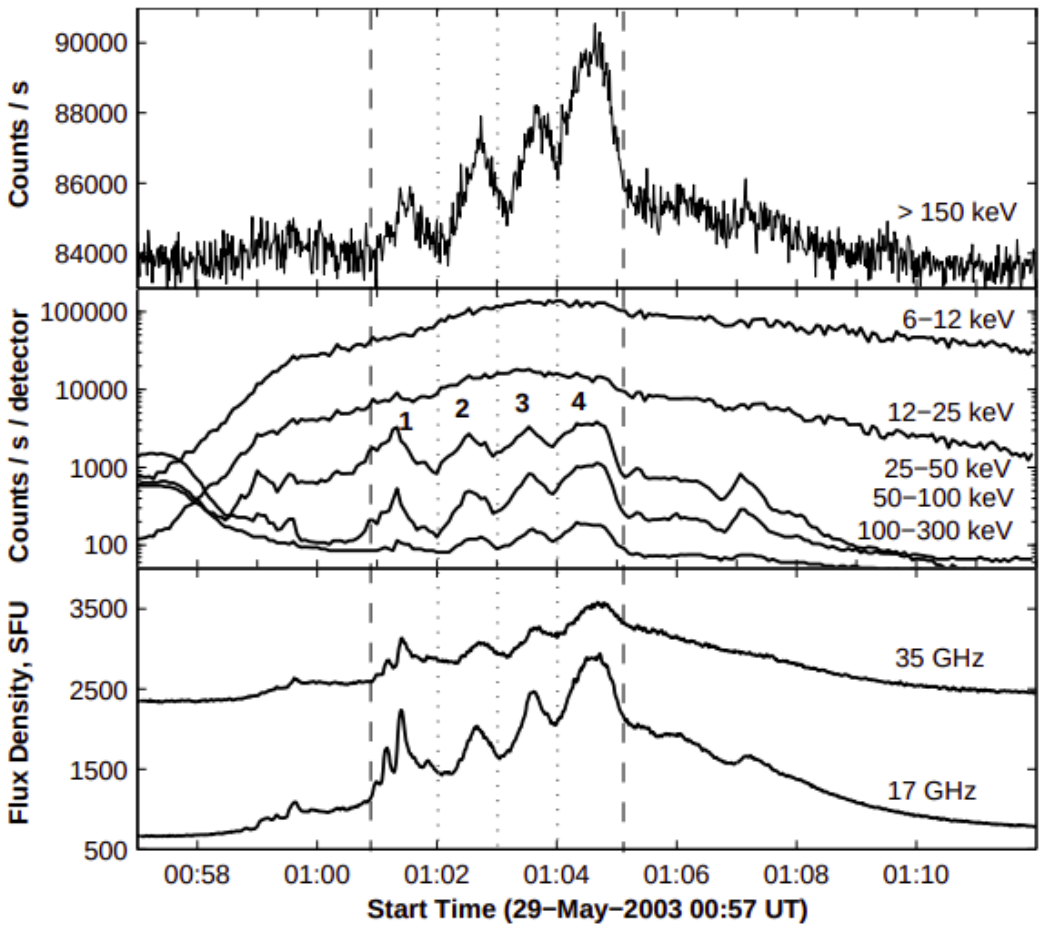

Figure 1.13: Examples of quasi-periodic pulsations (QPPs) observed in emission light curves of solar flares. The upper and middle panels depict QPPs in X-ray emissions, while the bottom panel displays the light curve in microwave emissions. These QPPs exhibit a periodicity of 1 minute (Credit: Zimovets and Struminsky (2009)).

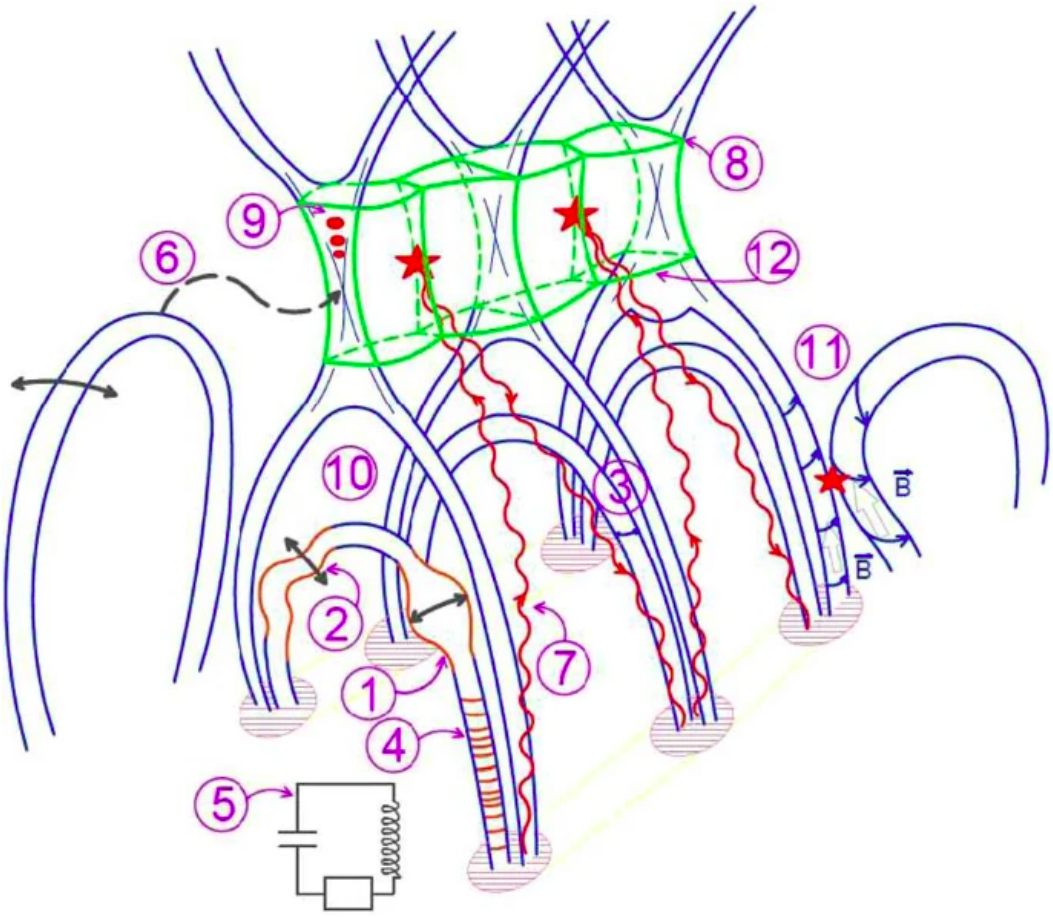

Figure 1.14: Diagrammatic representation of the principal models explaining QPPs (Credit: Kupriyanova et al. (2020)).

ongoing research, the exact formation mechanism of QPPs remains a subject of debate (e.g., Aschwanden, 1987; Nakariakov and Melnikov, 2009). In general, QPPs are believed to be associated with waves or energetic particles. Different types of MHD waves, such as fast kink, sausage kink, and slow magnetoacoustic waves are commonly suggested as explanations for QPPs.

It is essential to grasp the underlying physical mechanisms that give rise to quasi-periodic pulsations (QPPs) in solar flares. For this, McLaughlin et al. (2018), Kupriyanova et al. (2020), and (Zimovets et al., 2021) have proposed various interpretations. The detected periods indicate that QPPs originate from magnetohydrodynamic processes,

although it remains unclear whether they directly stem from coronal magnetic field oscillations. The frequency of detected QPPs increases with the solar cycle, corresponding to the heightened occurrence of flares. These QPPs exhibit diverse temporal behaviors, detectable through various measurement and observation techniques. rephrase completely. Figure 1.14 presents the primary physical processes employed for interpreting QPPs in solar flares. These models encompass processes such as sausage, kink, torsional Alfvén, slow magneto-acoustic modes, equivalent RLC circuit, periodic reconnection triggered by external waves, auto-wave processes, flapping oscillations, self-oscillatory processes, thermal over-stability, and periodic coalescence of two twisted loops, as well as the magnetic tuning fork model (Zimovets et al., 2021). Kupriyanova et al. (2020) categorize the physical processes into three groups, namely, modulation of direct emission by different types of magnetohydrodynamic (MHD) and electrodynamic oscillations, periodic modulation of energy release efficiency by MHD oscillations, and spontaneous quasi-periodic energy release. While certain mechanisms may fall into multiple categories, they aim to clarify the fundamental physical processes associated with each mechanism. In Chapter 6, we discussed the occurrence of Quasi-Periodic Pulsations (QPPs) during blowout jets. QPPs are a common phenomenon linked with solar and stellar flares, although their detection in solar jets is extremely uncommon. Multiple magnetic reconnections, like those seen in solar flares, can cause QPPs within a blowout jet (e.g., Morton et al., 2012). It is worth noting that QPPs in solar jets have not received significant attention in research, as there have been only a few documented instances of their presence. Furthermore, to the best of our knowledge, investigations into the relationship between solar jets, kink instability, and the formation of QPPs remain limited (Mishra et al., 2023; Morton et al., 2012).

1.6 Outline

In this thesis, we investigate the waves and oscillations occurring in the solar atmosphere. Wave heating plays a crucial role in coronal heating, prompting us to delve into various aspects of wave dynamics such as their generation, propagation, and dissipation in the solar atmosphere. Acoustic waves emerge from turbulent motion in the convection zone and extend into the photosphere, with plasma pressure acting as the restoring force. These waves lose energy as atmospheric properties change vertically in a stratified medium. Strong magnetic fields alter acoustic waves, turning them into slow magnetoacoustic waves. The solar corona is a focal point for sudden energy releases like jets, flares, and coronal mass ejections (CMEs), where oscillations and magnetohydrodynamic (MHD) waves are prevalent and vital for plasma heating. Typically, oscillations and waves in the solar atmosphere are observed through changes in intensity and Doppler shift over time. We analyze these changes to understand the periodicity and physical nature of these oscillations using wavelet and cross-wavelet analysis tools. In *Chapter 2*, we provide details about the instruments whose data we used in this thesis and describe the different data analysis techniques employed. In *Chapter 3*, we examine oscillations in the transition region above both network and inter-network regions in the quiet sun using IRIS data, analyzing intensity and Doppler shift time evolution and describing their physical nature. In *Chapter 4* we investigate wave propagation conditions above the inter-network region using multi-wavelength observations from IRIS, analyzing the simultaneous evolution of Doppler shift observed at different atmospheric heights. In *Chapter 5*, we study oscillations in the sunspot umbra using BBSO observational data, studying intensity oscillations in different passbands of the $H\alpha$ line and Doppler velocity oscillations, along with exploring the origin of these umbral oscillations. In *Chapter 6*, we examine quasi-periodic pulsations (QPPs) in solar coronal jets using imaging data from SDO/AIA and spectroscopic data from IRIS, investigating the mechanisms triggering QPPs. In *Chapter 7*, we summarize the

significance of the original research works presented in this thesis and outline the future plans.